Desalination and Water Treatment
www.deswater.com

doi: 10.5004/dwt.2019.23570

145 (2019) 361–368
March

Adsorption of Acid Red dye from aqueous solution using quaternized chitosan microspheres

Runhu Zhang[a], Chao Hua[b,*], Mencui Ning[a], Fang Bai[b]

[a]*Department of Chemical Engineering, Kunming Metallurgy College, Kunming 650033, China*
[b]*CAS Key Laboratory of Green Process and Engineering, Institute of Process Engineering, Chinese Academy of Sciences, Beijing 100190, China, email: huachao@ipe.ac.cn (C. Hua)*

Received 26 June 2018; Accepted 5 December 2018

ABSTRACT

In this study, quaternized chitosan microspheres (QCMS) were prepared and their adsorption performance of Acid Red 18 from aqueous solution was studied. Equilibrium was attained within 120 minutes and maximum removal of 94.06% was achieved. Langmuir and Freundlich isotherm models have been investigated. The maximum capacity obtained from the Langmuir model is 142.15 $mg \cdot g^{-1}$. Pseudo-first order and pseudo-second order kinetic models have been used for experimental data. The kinetic process was described by a pseudo-second-order rate equation very well. The calculated thermodynamic parameters ($\Delta H^\circ = -12.67$ $kJ \cdot mol^{-1}$; $\Delta G^\circ = -4.67$ to -5.61 $kJ \cdot mol^{-1}$ and $\Delta S^\circ = -24.78$ $K^{-1} \cdot mol^{-1}$) showed that the adsorption of Acid Red 18 is feasible, spontaneous and endothermic in nature. The results of the present study indicated that the QCMS could be considered as a potential adsorbent for Acid Red 18 in aqueous solutions.

Keywords: Acid Red 18; Quaternized chitosan microspheres; Adsorption; Isotherm models; Kinetics; Thermodynamics

1. Introduction

Dyes are widely used in textiles, dyeing, printing, electroplating, leather tanning, plastics, cosmetics, rubber, and food industries [1]. Industrial wastewaters from these industries are usually strongly colored, which may interfere with light penetration affecting the photosynthetic action [2]. In addition, some of the dyes are a threat to both aquatic life and human beings due to their toxicity, carcinogensis and mutagenicity. Azo dyes, which are characterized by nitrogen to nitrogen double bond (-N=N-), are easy to synthesize and have strong coloring ability. They are widely used in industries today because of its cost effectiveness compared to natural dyes. Azo dyes constitute 60–70% of synthetic dyes in the mentioned industries [3]. Azo dyes are difficult to be degraded because of the aromatic structure in the azo dye molecules. Therefore, how to effectively remove azo dyes from industrial wastewater has become extremely important to environmental safety [4–6]. In recent years, numerous methods have been developed to remove dyes from contaminated water, such as adsorption [7,8], biological degradation [9], photo-degradation [10], Fenton processes [11] electro-oxidation [12], reverse osmosis [13], ion exchange and so on [14]. However, most of these methods suffer from one or another limitation. Adsorption has proven to be as an effective, simple, and economically feasible method for removal of dyes from industrial wastewater.

Chitosan is a natural weakly alkaline polymer that is obtained by alkaline deacetylation of chitin. Chitosan has a large number of active amino and hydroxyl groups on the molecular chain. In addition, chitosan is nontoxic, biodegradable, polyfunctional and regenerable. Because of these properties, chitosan has been recognized as a promising raw material for adsorption purposes [15]. Many researchers have used chitosan as an adsorbent to remove heavy metals and dyes from wastewater and achieved great suc-

---

*Corresponding author.

1944-3994 / 1944-3986

cess [16,17]. However, Chitosan can be dissolved and lost in the acid condition, which is a disadvantage in the practical adsorption process. Quaternized chitosan has a positive charge and adsorption ability in a wide range of pH. Rosa et al. have investigated the adsorption of reactive orange 16 by cross-linked quaternized chitosan [18]. The results show that the adsorption process is independent on the pH value of the solution because it is the interaction of the sulfonate groups of active orange 16 with the polymer quaternary ammonium groups. Karthik [19] found that chitosan/polypyrrole composite was an effective adsorbent for the removal of Cr(VI) from aqueous solution. Wu et al. have have prepared EDTA modified β-cyclodextrin/chitosan (CDCS-EDTA) and applied them to remove Pb(II) and anionic dye acid red 73 (AR) [20].

Based on the best of our knowledge, the use of quaternized chitosan microspheres (QCMS) for removing Acid Red18 was not presented in the literature. Acid Red 18 (AR18) was selected as the model adsorbate because it is widely used in the textile, paper and leather industries. In this study, the quaternized chitosan microspheres were prepared and tested for their potential ability to remove acid red 18 (AR18) from aqueous solution. Several operating parameters affecting the sorption process such as contact time, temperature, pH and adsorbent dose were also studied. In addition, the observed data were analyzed by different kinetic and isotherm models. Thermodynamic parameters such as enthalpy change (ΔH°), free energy change (ΔG°),and entropy change (ΔS°) for sorption process were evaluated.

2. Materials and methods

2.1. Materials and analytical method

Chitosan (degree of deacetylation 85%) was purchased from Jinan Haidebei Marine Bioengineering Co. Ltd. The Acid Red 18 purchased from National Medicine Group Chemical Reagent Co., Ltd. was used as adsorbate in the tests. All of the other reagents were used as received from the suppliers without any further purification. An aqueous stock solution of Acid Red 18 was prepared by dissolving a specified amount of Acid Red 18 in 1000 mL of deionized water, and subsequently diluted to other working solutions with different concentration. The concentration of the AR18 solution was measured by using a UV-Visible spectro-photometer (Shimadzu UV 1601) at its maximum absorption wavelength of 506 nm [21].

The Acid Red 18 adsorbed per unit mass of adsorbent, q_e and q_t were calculated by using the following mass balance equation:

$$q_\mathrm{e} = \frac{\left(C_0 - C_e\right)V}{W} \tag{1}$$

$$q_\mathrm{t} = \frac{\left(C_0 - C_t\right)V}{W} \tag{2}$$

where q_t is the amount of Acid Red 18 adsorbed at time t (mg g^{-1}), and q_e is the amount of Acid Red 18 adsorbed at equilibrium (mg g^{-1}). C_0 is an initial concentration of Acid Red 18 (mg L^{-1}), C_e is the equilibrium concentration of Acid Red 18 (mg L^{-1}). V is the solution volume (L), and W is the amount of the adsorbent (g).

2.2. Preparation of adsorbents

5.0 g chitosan powders were dissolved in thoroughly 100 mL of 2% (W/V) acetic acid under stirring at room temperature, and then 0.03 g of PEG 2000 was added and stirred to produce a large number of small bubbles. Subsequently, the mixture was added with a syringe in the dispersion medium, consisting of 160 mL of paraffin oil and 3.0 mL of Span 80, under stirring condition. Then, 6.7 mL of formaldehyde was added and the solution was stirred for another 1 h to protect the amino group. After 1 h of stirring, the mixture was poured into 200 mL NaOH ethanol solution (10% NaOH/95% ethanol, vol/vol, 1:1) and stirred for 2 h. The products were collected by suction filtered carefully and washed thoroughly with petroleum ether and ethanol. The obtained chitosan microspheres were transferred into a three-necked flask with 0.4 mol·L^{-1} NaOH solution. Next, an aqueous solution of 3-chloro-2-hydroxypropyltrimethyl ammonium chloride (CHPTAC) was added to the reaction mixture. The mixture was stirred for 8 h at 60°C to allow for the crosslinking reaction to occur. The products were washed using distilled water and suspended in 0.5 M HCl for 12 h to remove the protective group. Subsequently, the products were filtered and dried in vacuum at 45°C to produce quaternized chitosan microspheres.

2.3. Characterization of the adsorbents

The Scanning electron microscopic (SEM) of the QCMS was carried out using scanning electron microscopy (Hitachi S-3500N, Hitachi company, JPN). The Fourier transform infrared (FTIR) spectra of the chitosan, QCMS before and after the adsorption were recorded on a FTIR Spectrometer (Nexus 470, Thermo Nicolet,USA) using KBr pellets over the rang 4000–400 cm^{-1}. XRD patterns of the chitosan and QCMS were obtained by an X-ray diffractometer (XRD-7000, Shimadzu, Shimadzu Corporation, Kyoto, Japan).

2.4. Adsorption experiments

Batch adsorption experiments were done by varying contact time, pH , adsorbent dose,temperature, and adsorbate concentration. The pH effect on adsorption was determined by using 0.05 g of quaternized chitosan microspheres, 100 mL of 150 mg L^{-1} Acid Red 18 solution, at temperature of 25± 1°C and various pH values ranging from 1 to 12. 0.1 M HCl and NaOH solutions were used to adjust the pH over the range 1.0–12. The mixture was shaken for 2 h, and the solution was filtered and analysed. For optimization of contact time, the contact time was varied between 10 and 120 min, keeping all the remaining variables constant. The effect of adsorbent dosage on dye removal was investigated by adding 0.02–0.14 g of adsorbent into 100 mL solution of Acid Red 18 with a concentration of 50 mg L^{-1} .

Adsorption at equilibrium was performed by adding 0.05 g of quaternized chitosan microspheres into 100 mL of Acid Red 18 solution with varying initial concentrations from 50 mg/L to 250 mg/L, and shaken at 20°C for 2 h. The kinetic experiments were conducted by using 0.05 g of quaternized chitosan microspheres and Acid Red 18 dye solution with various concentrations whereas contact time was varied from 10 to 120 min at room temperature. Finally, The adsorption thermodynamics were studied at 20–50°C by using a 100 mL dye solution (150 mg/L) and 0.05 g of adsorbent dosage at pH 7.0 for 2 h.

3. Results and discussion

3.1. Sorbent characterization

Fig. 1 shows a general SEM micrograph of the QCMS, and it can clearly be seen that the QCMS are well shaped spheres. The QCMS have the diameter size range of 1 μm–5 μm. Fig. 2 shows the FT-IR spectra of chitosan, the QCMS and after QCMS adsorption. In chitosan obvious translocations are observed at 3500–3200 cm^{-1} due to O–H and N–H group. The peak at 2928 cm^{-1} and 2878 cm^{-1} was attributed to the stretching vibration of $-CH_3$ and $-CH_2$ group. The peak at 1595 cm^{-1} is the N–H$_2$ deformation vibration of amino groups. Compared to chitosan, the peak at 1595 cm^{-1} disappears in the QCMS. The peak at 1573 m^{-1} is the N–H$_2$ deformation vibration of amino groups. The peak at 1474 cm^{-1} is assigned to asymmetric CH stretching vibration of quaternary ammonium salts. The peak at 971 cm^{-1} is assigned to absorption peak of quaternary ammonium salt [22]. The above analyses indicated that the adsorbent (QCMS) had been successfully prepared. In the FT-IR spectra of the QCMS loaded with Acid Red 18, new peaks appearing at 1210 cm^{-1} and 1459 cm^{-1} were attributed to the SO$_3$ of dye and the ring of dye. These peaks confirmed the attachment of Acid Red 18 on the QCMS.

Fig. 3 indicates the XRD patterns of chitosan and the QCMS. It can be seen from Fig. 3 that chitosan has two distinct diffraction peaks 2θ = 12°and 2θ = 20.8°. Compared with chitosan, the diffraction peak of the QCMS is flat and wide, which indicates that the structurally of QCMS destroys a large number of hydrogen bonds in its molecular structure, which makes the crystal structure from stereotyped to amorphous, and the crystallinity decreases. The BET surface area was 4.45 m^2/g. Average pore width was measured 0.5 μm. Volume of pores were 0.0186 cm^3/g.

3.2 Effect of contact time

Fig. 4 demonstrates the effect of contact time on the adsorption of Acid Red 18. Where it can be seen intuitively that adsorption of Acid Red 18 increases sharply

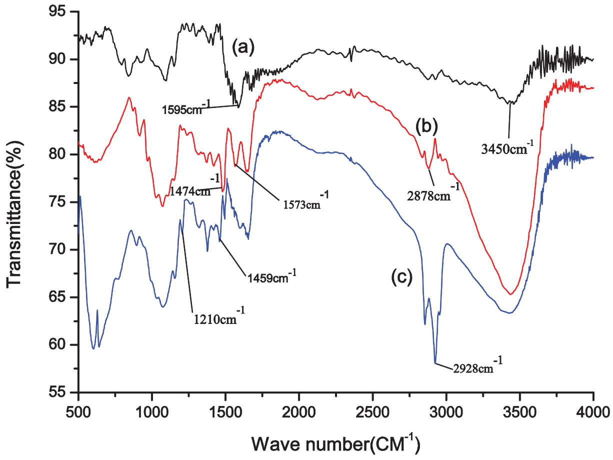

Fig. 2. FTIR spectra of chitosan (a), the QCMS (b) and the QCMS loaded with Acid Red 18 (c).

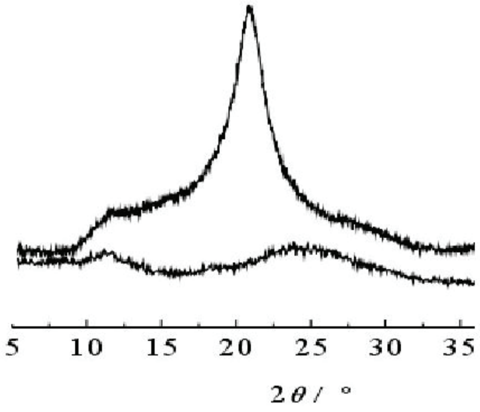

Fig. 3. X-ray diffraction patterns of chitosan and the QCMS.

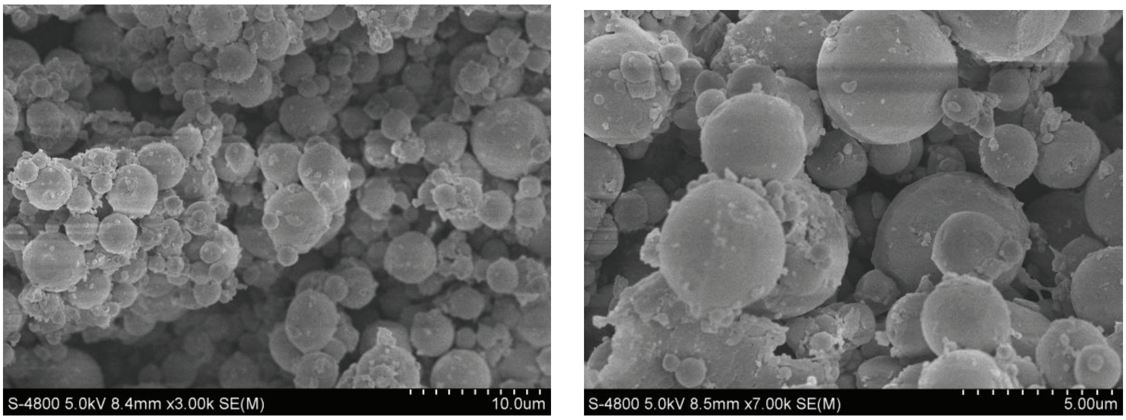

Fig. 1. SEM images of the QCMS.

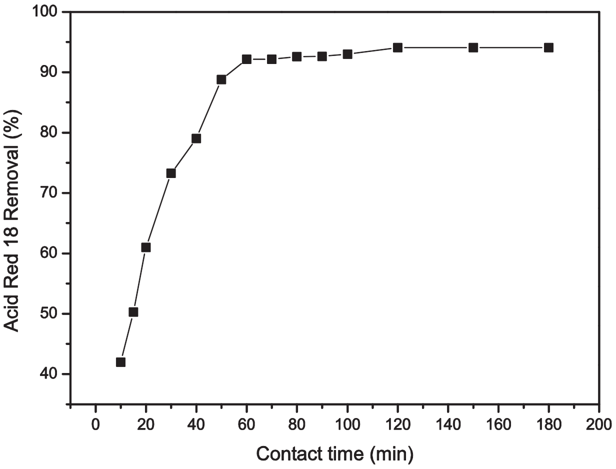

Fig. 4. Effect of contact time on Acid Red 18 removal.

with time in the first 60 min. Thereafter, the percentage removal of Acid Red 18 increases slowly with the prolongation of contact time. This behavior can be attributed to the abundant availability of active binding sites for adsorption in the initial stage. Then, with gradual occupancy of these sites, the available sites become fewer in the later stages. Observed removal efficiency was 94.06% at 120 min. The adsorption reached equilibrium in about 120 min. The removal efficiency after 120 min became almost constant. Thus, this value was selected as the optimum contact time.

3.3. Effect of pH

The effect of the initial solution pH (1.0–12.0) on removal of Acid Red 18 from aqueous solution is shown in Fig. 5. Accordingly, the percentage of dye removal is maintained at a high level in the range of pH from 1 to 10, and the value is higher than 82%. The maximum percent removal was obtained at pH 8.4. Above a pH of 9, the percentage of dye removal began to decrease. The Acid Red 18 were negatively charged even in highly acid solutions due to the N=N bonds and sulfonic groups [23].

The main reasons may be as follows: At pH < 9, there are electrostatic attractions between the anionic dye and the functional groups of quaternized chitosan microspheres. At pH < 10, abundant presence of hydroxyl ions can compete with the dye for adsorption sites.

3.4 Effect of adsorbent dosage

The effect of adsorbent dosage on the removal of Acid Red 18 is presented in Fig. 6. As clearly shown from Fig. 6, the removal percentage of Acid Red 18 increased significantly with the increase in adsorbent dosage until a certain value was reached. This can be attributed to the availability of larger surface area and more adsorption sites. Above this value, the removal efficiency remained constant even if the quaternized chitosan microspheres were added. This may be due to the saturation of the available active sites of the adsorbent.

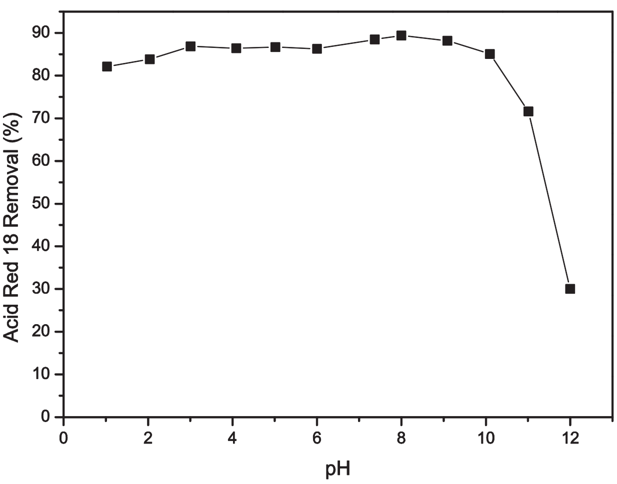

Fig. 5. Influence of initial pH on Acid Red 18 removal.

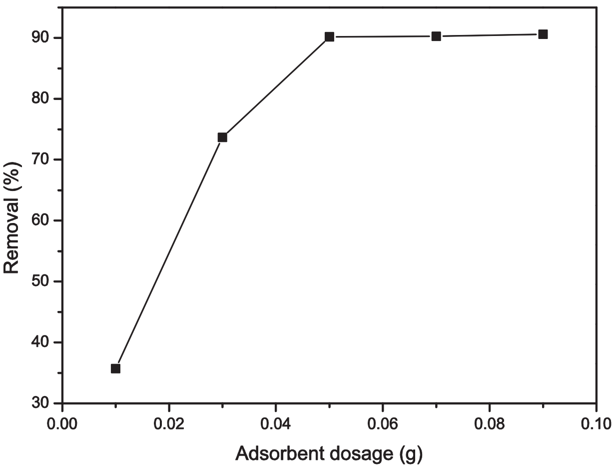

Fig. 6. Dependence of Acid Red 18 adsorption on the amount of adsorbent.

3.5. The adsorption isotherm

To investigate the sorption isotherms, the two most common models, Langmuir and Freundlich isotherm equations [24,25] were applied to understand the adsorption data.

The linearised forms of isotherm equations are expressed as the following:

Langmuir:

$$\frac{C_e}{q_e} = \frac{C_e}{Q_o} + \frac{1}{Q_o b} \tag{3}$$

Freundlich:

$$\log q_e = \log K + \frac{1}{n}\log C_e \tag{4}$$

where Q_0 and b are the Langmuir constants related to the sorption capacity and the rate of adsorption, respectively. C_e is the equilibrium liquid phase concentration (mg L^{-1}), and q_e is the amount of sorbent adsorbed per unit weight (mg g^{-1}); K and n are Freundlich equilibrium coefficients related to the adsorption capacity and the heterogeneity factor .

The favorable or unfavorable of the adsorption system can be determined based on a dimensionless equilibrium parameter, R_L [26], which is given by the following equation:

$$R_L = \frac{1}{1+bC_0} \tag{5}$$

where C_0 (mg L^{-1}) is the initial Acid Red 18 concentration, and b (L mg^{-1}) is the Langmuir constant. The value of R_L lies between 0 and 1 for a favorable adsorption, while $R_L > 1$ represents an unfavorable adsorption, and $R_L = 1$ represents the linear adsorption, while the adsorption operation is irreversible if $R_L = 0$.

The curves related to the Langmuir and Freundlich models are shown in Figs. 7, 8, respectively. Isotherm parameters of the both models along with the regression coefficients are reported in Table 1. The adsorption isotherm data of Acid Red 18 on this adsorbent are best fitted to Langmuir isotherm and Freundlich model. The regression coefficient of Freundlich model is 0.9972. The values of the constants K and n were calculated to be 21.64 and 1.18 respectively. In all cases, the value of n between 1 and 10 shows beneficial adsorption, while the relatively low K value suggests that a lesser number of active sites are available. The regression coefficient of Langmuir model is 0.9981. Q_0 and b were determined to be 142.15 (mg g^{-1}) and 0.12 (L mg^{-1}), respectively. For comparative purposes, the absorbability of Acid Red 18 onto different adsorbents is also listed in Table 2. The results show that the QCMS possesses a large adsorption capacity in comparison with other sorbents.

R_L values at different initial dye concentrations are 0.032, 0.039, 0.052, 0.076 and 0.142. These values are much less than 1 and very close to 0. Therefore, the sorption process is very favorable and the adsorbent employed exhibits a good potential for the removal of Acid Red 18 from aqueous solution [27].

3.6. Thermodynamic parameters

Thermodynamic parameters including the changes in entropy (ΔS°), enthalpy (ΔH°) and free energy (ΔG°) were calculated by using the following equations [28,29]:

$$Kc = \frac{C_{Ae}}{C_e} \tag{6}$$

$$\ln K_c = -\frac{\Delta H^\circ}{RT} + \frac{\Delta S^\circ}{R} \tag{7}$$

$$\Delta G^\circ = \Delta H^\circ - T\Delta S^\circ \tag{8}$$

where K_c is the adsorption equilibrium constant, C_e is the equilibrium concentration (mg L^{-1}) of Acid Red 18 in the solution, and C_{Ae} is the amount of Acid Red 18 (mg) adsorbed on the adsorbent per liter of the solution at equilibrium. R is the universal gas constant (8.314 J/mol K), and T is the absolute temperature (in Kelvin).

The values of ΔH° and ΔS° were determined from the slope and intercept by plotting a graph of log K_c versus 1/T

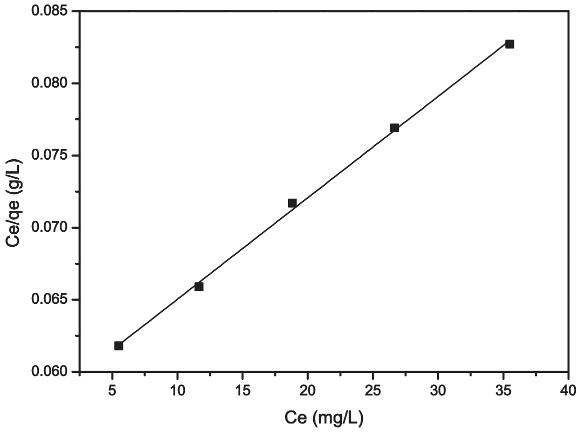

Fig. 7. Langmuir adsorption isotherm for Acid Red 18 adsorption on QCMS.

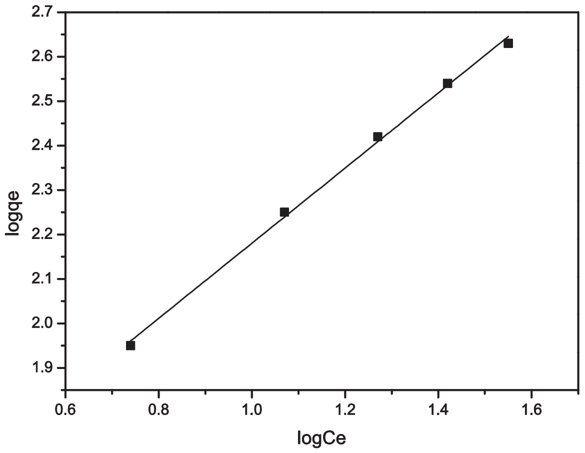

Fig. 8. Freundlich adsorption isotherm for Acid Red 18 adsorption on QCMS.

Table 1
Parameters of the Langmuir and Freundlich isotherm models

T (K)	Langmuir			Freundlich		
	Q_0 (mg g^{-1})	b (L mg^{-1})	R^2	K (mg g^{-1}) (L mg^{-1})$^{1/n}$	n	R^2
293	142.15	0.12	0.9981	21.64	1.18	0.9972

Table 2
The adsorptive capacities of various adsorbents for Acid Red 18

Adsorbent	Q_0 (mg g^{-1})	pH	Reference
Modified magnetite nanoparticles	73.46	3.0	[34]
Modified biochars	134.17	6.6	[35]
AC prepared from walnut woods	30.30	5.0	[36]
Polyaniline-modified rice husk	100.00	3.0	[37]
Bentonite based composite adsorbent	69.80	–	[38]
QCMS	142.15	8.4	This work

(Fig. 9). The obtained values are listed in Table 3. The negative values of the Gibbs-free energy change are acquired at all temperatures, which indicate that the adsorption process is spontaneous. The negative value of ΔH° (–12.67 kJ mol^{-1}) is due to the exothermic nature of adsorption of Acid Red 18 on the quaternized chitosan microspheres. In other words, the high temperature is unfavorable to the progress of adsorption. The entropy change (ΔS°) is –-24.78 J·mol^{-1}·K^{-1}, the negative value of ΔS° reveals the decreased randomness during the removal of Acid Red 18 dye on quaternized chitosan microspheres [30,31].

The values of enthalpy change can give some insight into the bonding mechanism. In general, the enthalpy change of physical adsorption is less than that of chemical adsorption. The magnitude of the ΔH° value lies in the range of 20–40 kJ·mol^{-1} and 80–400 kJ·mol^{-1} for physical and chemical adsorptions, respectively. The change of enthalpy indicated that the adsorption process is essentially physical adsorption.

3.7. Adsorption kinetics

Two well-known kinetic models were used to examine the mechanism of the adsorption process: Lagergren pseudo-first-order and Ho pseudo-second-order equations [32,33].

Lagergren pseudo-first-order:

$$\log(q_e - q_t) = \log(q_e) - \frac{k_1}{2.303}t \tag{9}$$

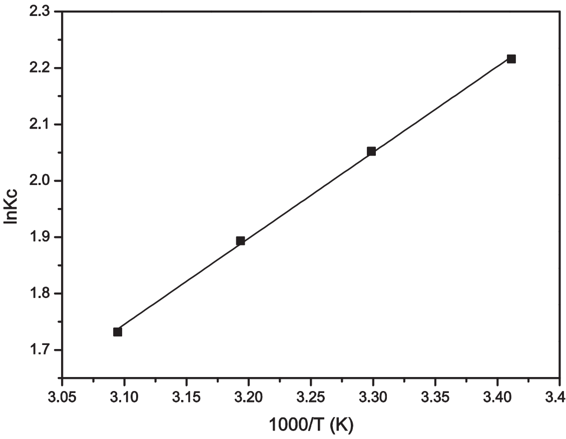

Fig. 9. Plot of log K_c vs. 1/T for Acid Red 18 adsorption on QCMS.

Table 3
Thermodynamic parameters for adsorption of Acid Red 18 on QCMS

Temperature (K)	ΔG^O (kJ·mol^{-1})	ΔH^O (kJ·mol^{-1})	ΔS^O (J·mol^{-1}·K^{-1})
293	–5.41	–12.67	–24.78
303	–5.16		
313	–4.91		
323	–4.67		

Ho pseudo-second-order:

$$\frac{t}{q_t} = \frac{1}{k_2 q_e^2} + \frac{1}{q_e}t \tag{10}$$

where q_t and q_e are the amount of Acid Red 18 adsorbed (mg g^{-1}) at time t and at equilibrium, respectively; k_1 (min^{-1}) and k_2 (mg g^{-1}·min^{-1}) are the pseudo-first-order and Ho pseudo-second-order rate constants.

For the pepseudo- first-order equation, a plot of log (q_e – q_t) vs. t for sorption of Acid Red 18 is shown in Fig. 10. The application of pseudo-second-order equation by plotting t/q_t vs. t is shown Fig. 11. The kinetic constants and correlation coefficients R^2 for the models are listed in Table 4. Based on the correlation coefficients R^2, the experimental data fit to the pseudo-second-order model (R^2 > 0.99) better than to the pseudo-first-order model. Similar results have been observed in the adsorption of reactive orange 16 onto quaternary chitosan [18].

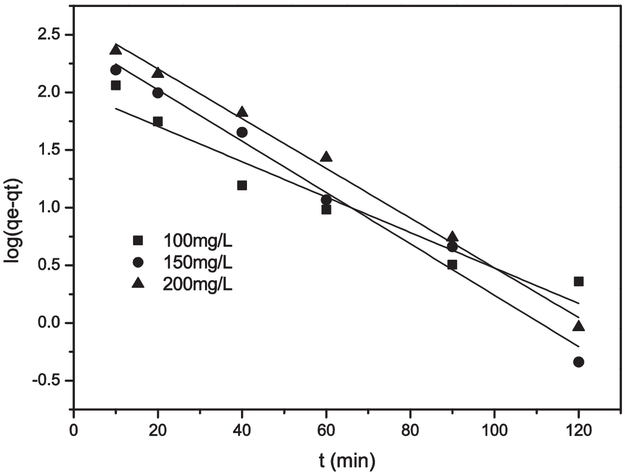

Fig. 10. Lagergren first-order kinetic plot for the sorption of Acid Red 18 on QCMS.

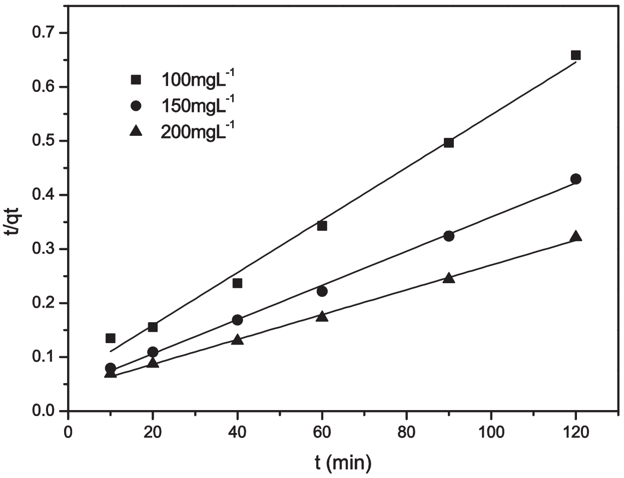

Fig. 11. Second-order kinetic plot for the sorption of Acid Red 18 on QCMS.

Table 4
Kinetic parameters for pseudo-first order and pseudo-second order

Pseudo-first order				Pseudo-second order		
C_0 (mg L^{-1})	K_1 (min^{-1})	q_{e1} (mg.g^{-1})	R^2	K_2 (g.mg^{-1}.min^{-1})	q_{e2} (mg.g^{-1})	R^2
100	0.03537	102.3	0.9176	3.8×10^{-4}	205.3	0.9922
150	0.05128	288.4	0.9808	2.3×10^{-4}	316.46	0.9971
200	0.04967	426.5	0.9923	1.3×10^{-4}	434.8	0.9972

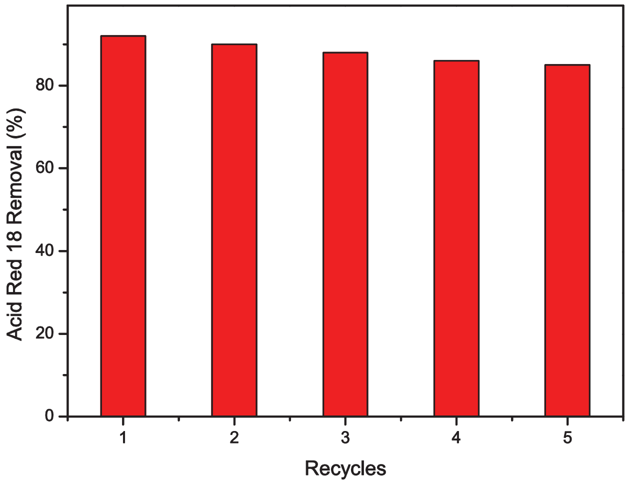

Fig. 12. Regeneration studies of QCMS for Acid Red 18 over five cycles.

3.8. Desorption and reusability

The recycling performance of the adsorbent is critical in the dye wastewater treatment process. In this study, 0.1 mol L^{-1} NaOH was used for the desorption of Acid Red 18. The cyclic regeneration performance of QCMS for the Acid Red 18 is shown in Fig. 12. It can be seen from Fig. 11 that after five cycles of regeneration, the removal rate of the dye by the adsorbent can still be maintained above 85%. Therefore, QCMS has good adsorption performance and high chemical stability.

4. Conclusions

Chitosan has excellent properties for wastewater treatment. In this study, the quaternized chitosan microspheres were successfully prepared, characterized and used to remove Acid Red 18. Adsorption equilibrium was attained within a contact time of 120 min. It was found that the quaternized chitosan microspheres efficiently removed Acid Red 18 in a range of pH of 1–10, this being an advantage for practical applications. The optimum pH value was found to be 8.4. Experimental isotherms of Acid Red 18 were successfully fit to the Langmuir and Freundlich models, with good correlation coefficients. Value of Q_0 was obtained as 142.15 mg g^{-1} at 20°C. The values of ΔH° and ΔG°confirmed the exothermic and spontaneous character of adsorption process. The kinetic data of Acid Red 18 were best described by pseudo-second-order model. The quaternized chitosan microspheres proved to be effective for Acid Red 18 removals, thus having a strong potential for application in the treatment of effluents.

Acknowledgement

This work was financially supported by the national key basic research development plan (973) funded projects (No.2013CB632602).

References

[1] Z. Hasan, S.H. Jhung, Removal of hazardous organics from water using metal-organic frameworks (MOFs): Plausible mechanisms for selective adsorptions, J. Hazard. Mater., 283 (2015) 329–339.
[2] C.M. Kao, M.S. Chou, W.L. Fang, B.W. Liu, B.R. Huang, Regulating color textile wastewater by 3/31 wavelength admi methods in Taiwan, Chemosphere, 44 (2001) 1055–1063.
[3] E. Hosseini Koupaie, M. Alavi Moghaddam, S. Hashemi, Post-treatment of anaerobically degraded azo dye Acid Red 18 using aerobic moving bed biofilm process: enhanced removal of aromatic amines, J. Hazard. Mater., 195 (2011) 147–154.
[4] H. Tajizadegan, M. Jafari, M. Rashidzadeh, A. Saffar-Teluri, A high activity adsorbent of ZnO–Al_2O_3 nanocomposite particles: synthesis, characterization and dye removal efficiency, Appl. Surf. Sci., 276 (2013) 317–322.
[5] A.Y. Dursun, O. Tepe, Removal of Chemazol Reactive Red 195 from aqueous solution by dehydrated beet pulp carbon, J. Hazard. Mater., 194 (2011) 303–311.
[6] M.F. Zhao, Z.B. Tang, P. Liu, Removal of methylene blue from aqueous solution with silica nano-sheets derived from vermiculite, J. Hazard. Mater., 158 (2008) 43–51.
[7] M. Auta, B.H. Hameed, Coalesced chitosan activated carbon composite for batch and fixed-bed adsorption of cationic and anionic dyes, Colloids Surf. B, 105 (2013) 199–206.
[8] S.E. Subramani, N. Thinakaran, Isotherm, kinetic and thermodynamic studies on the adsorption behavior of textile dyes onto chitosan, Process Saf. Environ. Prot., 106 (2016) 1–10.
[9] Z. Khan, K. Jain, A. Soni, D. Madamwar, Microaerophilic degradation of sulphonated azo dye Reactive Red 195 by bacterial consortium AR1 through co-metabolism, Int. Biodeterior. Biodegrad., 94 (2014) 167–175.
[10] S. Sabar, M.A. Nawi, W.S.W. Ngah, Photocatalytic removal of Reactive Red 4 dye by immobilised layer-by-layer TiO_2/cross-linked chitosan derivatives system, Desal. Water Treat., 57 (2016) 5851–5857.
[11] Y. Liu, W. Jin, Y. Zhao, G. Zhang, W. Zhang, Enhanced catalytic degradation of methylene blue by α-Fe_2O_3/graphene oxide via heterogeneous photo-Fenton reactions, Appl. Catal., B, 206 (2017) 642–652.
[12] K. Rajkumar, M. Muthukumar, Optimization of electro-oxidation process for the treatment of Reactive Orange 107 using response surface methodology, Environ. Sci. Pollut. Res., 19 (2012) 148–160.
[13] S.K. Nataraj, K.M. Hosamani, T.M. Aminabhavi, Nanofiltration and reverse osmosis thin film composite membrane module for the removal of dye and salts from the simulated mixtures, Desalination, 249 (2009) 12–17.
[14] S.S. Behera, S. Das, P.K. Parhi, S.K. Tripathy, R.K. Mohapatra, Kinetics, thermodynamics and isotherm studies on adsorption of methyl orange from aqueous solution using ion exchange resin Amberlite IRA-400, Desal. Water Treat., 60 (2017) 249–251.
[15] C.M. Futalan, C.C. Kan, M.L. Dalida, K.J. Hsien, C. Pascua, M.W. Wan, Comparative and competitive adsorption of copper, lead, and nickel using chitosan immobilized on bentonite, Carbohyd. Polym., 83 (2011) 528–536.

[16] G.G. Maghami, G.A. Roberts, Studies on the adsorption of anionic dyes on chitosan, Makromol. Chem., 189 (1988) 2239–2243.

[17] A. Kamari, W.S.W. Ngah, Removal of cadmium using chitosan, Colloid. Surf. B: Biointerf., 73 (2009) 257–266.

[18] S. Rosa, M.C. Laranjeira, H.G. Riela, V.T. Fávere, Cross-linked quaternary chitosan as an adsorbent for the removal of the reactive dye from aqueous solutions, J. Hazard. Mater., 155 (2008) 253–260.

[19] R. Karthik, S. Meenakshi, Removal of hexavalent chromium ions from aqueous solution using chitosan/polypyrrole composite, Desal. Water Treat., 56(6) (2015) 1587–1600.

[20] D. Wu, L. Hu, Y. Wang, Q. Wei, L. Yan, T. Yan, Y. Li, B. Du, EDTA modified β-cyclodextrin/chitosan for rapid removal of Pb(II) and acid red from aqueous solution, J. Colloid Interface Sci., 523 (2018) 56–64.

[21] N. Mirzaei, M. Hadi, M. Gholami, R.F. Fard, M.S. Aminabad, Sorption of acid dye by surfactant modificated natural zeolites, J. Taiwan Inst. Chem. Eng., 59 (2016) 186–194.

[22] C. Hua, R.h. Zhang, F. Bai, P. Lu, X.f. Liang, Removal of chromium (VI) from aqueous solutions using quaternized chitosan microspheres, Chin. J. Chem. Eng., 25 (2017) 153–158.

[23] Y.C. Wong, Y.S. Szeto, W.H. Cheung, G. McKay, Adsorption of acid dyes on chitosan - equilibrium isotherm analyses, Process Biochem., 39 (2004) 693–702.

[24] I. Langmuir, The constitution and fundamental properties of solids and liquids, J. Am. Chem. Soc., 38 (1916) 2221–2295.

[25] H. Freundlich, Uber die adsorption in losungen, Zeitsch. Phys. Chem., 57 (1906) 385–470.

[26] K.R. Hall, L.C. Eagleton, A. Acrivos, T. Vermeulen, Pore and solid diffusion kinetics in fixed bed adsorption under constant pattern conditions, Ind. Eng. Chem. Fundam., 5 (1966) 212–223.

[27] A.K. Bhattacharya, S.N. Mandal, S.K. Das, Adsorption of Zn(II) from aqueous solution by using different adsorbents, Chem. Eng. J., 123 (2006) 43–51.

[28] Y.S. Ho, Removal of copper ions from aqueous solution by tree fern, Water Res., 37 (2003) 2323–2330.

[29] K.K. Singh, A.K. Singh S.H. Hasan, Low cost biosorbent wheat bran for the removal of cadmium from wastewater: Kinetic and equilibrium studies, Bioresour. Technol., 97 (2006) 994–1001.

[30] A. Sari, M. Tuzen, Removal of Cr(VI) from aqueous solution by Turkish vermiculite: equilibrium, thermodynamic and kinetic studies, Sep. Sci. Technol., 43 (2008) 3563–3581.

[31] M.S. Gasser, G.H.A. Morad, H.F. Aly, Batch kinetics and thermodynamics of chromium ions removal from waste solutions using synthetic adsorbents, J. Hazard. Mater., 142 (2007) 118–129.

[32] W. Rudzinski, W. Plazinski, Kinetics of solute adsorption at solid/solution interfaces: A theoretical development of the empirical pseudo-first and pseudo second-order kinetic rate equations, based on applying the statistical rate theory of interfacial transport, J. Phys. Chem. B., 110 (2006) 16514–16525.

[33] Y.S. Ho, G. McKay, The kinetics of sorption of divalent metal ions onto sphagnum moss peat, Water Res., 34 (2000) 735–742.

[34] Z. Berizi, S.Y. Hashemi, M. Hadi, A. Azari, A.H. Mahvi, The study of non-linear kinetics and adsorption isotherm models for Acid Red 18 from aqueous solutions by magnetite nanoparticles and magnetite nanoparticles modified by sodium alginate, Water Sci. Technol., 74 (2016) 1235–1242.

[35] L. Wang, W. Yan, C. He, H. Wen, Z. Cai, Z.x. Wang, Z.Z. Chen, W.F. Liu, Microwave-assisted preparation of nitrogen doped biochars by ammonium acetate activation for adsorption of acid red 18, Appl. Surf. Sci., 433 (2018) 222–231.

[36] B. Heibati, S. Rodriguez-Couto, M.A. Al-Ghouti, M. Asif, I. Tyagi, S. Agarwal, V. K.r Gupta, Kinetics and thermodynamics of enhanced adsorption of the dye AR 18using activated carbons prepared from walnut and poplar woods, J. Mol. Liq., 208 (2015) 99–105.

[37] M. Shabandokht, E. Binaeian, H. Tayebi, Adsorption of food dye Acid red 18 onto polyaniline-modified rice husk composite: isotherm and kinetic analysis, Desal. Water Treat., 57 (2016) 27638–27650.

[38] S.Z. Qiao, Q.H. Hua, F. Haghseresht, X.J. Hu, G.Q. Lua, An investigation on the adsorption of acid dyes on bentonite based composite adsorbent, Sep. Purif. Technol., 67 (2009) 218–225.